Received: 27 September 2021 | Revised: 24 March 2022 | Accepted: 25 March 2022

DOI: 10.1111/mmi.14901

RESEARCH ARTICLE

WILEY

The novel protein ScrA acts through the SaeRS two-component system to regulate virulence gene expression in *Staphylococcus aureus*

Marcus A. Wittekind[1] | Andrew Frey[2] | Abigail E. Bonsall[1] | Paul Briaud[1] | Rebecca A. Keogh[1] | Richard E. Wiemels[1] | Lindsey N. Shaw[2] | Ronan K. Carroll[1,3]

[1]Department of Biological Sciences, Ohio University, Athens, Ohio, USA

[2]Department of Cell Biology, Microbiology & Molecular Biology, University of South Florida, Tampa, Florida, USA

[3]Infectious and Tropical Disease Institute, Ohio University, Athens, Ohio, USA

Correspondence
Ronan K. Carroll, Department of Biological Sciences, Ohio University, Ronan Carroll, 107 Irvine Hall, Athens, OH 45701, USA.
Email: carrolr3@ohio.edu

Present address
Rebecca A. Keogh, Department of Immunology & Microbiology, University of Colorado School of Medicine, Aurora, Colorado, USA

Funding information
National Institute of Allergy and Infectious Diseases, Grant/Award Number: AI124458, AI156391 and AI157506; Ohio University

Abstract

Staphylococcus aureus is a Gram-positive commensal that can also cause a variety of infections in humans. *S. aureus* virulence factor gene expression is under tight control by a complex regulatory network, which includes, sigma factors, sRNAs, and two-component systems (TCS). Previous work in our laboratory demonstrated that overexpression of the sRNA tsr37 leads to an increase in bacterial aggregation. Here, we demonstrate that the clumping phenotype is dependent on a previously unannotated 88 amino acid protein encoded within the tsr37 sRNA transcript (which we named ScrA for *S. aureus* clumping regulator A). To investigate the mechanism of action of ScrA we performed proteomics and transcriptomics in a ScrA overexpressing strain and show that a number of surface adhesins are upregulated, while secreted proteases are downregulated. Results also showed upregulation of the SaeRS TCS, suggesting that ScrA is influencing SaeRS activity. Overexpression of ScrA in a *saeR* mutant abrogates the clumping phenotype confirming that ScrA functions via the Sae system. Finally, we identified the ArlRS TCS as a positive regulator of *scrA* expression. Collectively, our results show that ScrA is an activator of the SaeRS system and suggests that ScrA may act as an intermediary between the ArlRS and SaeRS systems.

KEYWORDS
SaeRS, small proteins, *Staphylococcus aureus*, virulence

1 | INTRODUCTION

Staphylococcus aureus is a gram-positive opportunistic pathogen capable of causing a wide variety of diseases ranging from minor skin and soft tissue infections to life-threatening endocarditis and bacterial septicemia (Tong et al., 2015). *S. aureus* is regarded as a human commensal with approximately 27% of the population being colonized in the nares (Wertheim et al., 2005). Colonization with *S. aureus* is usually asymptomatic, however, colonized individuals are at greater risk for *S. aureus* invasive infections (Kluytmans et al., 1997; Wertheim et al., 2005). The versatility of *S. aureus*, in terms of lifestyle and severity of infection, is due in part to the arsenal of virulence factors encoded by the bacterium. Amongst these virulence factors are adhesins, toxins, exoenzymes, and immune evasion proteins. Precise, coordinated expression of the genes encoding these virulence factors is critical for *S. aureus* to cause disease, and

a complex network of regulatory circuits has been implicated in the regulation of virulence gene expression.

Two-component signal transduction systems (TCS) are well-characterized virulence regulators in *S. aureus*. There are 16 two-component systems encoded on the *S. aureus* genome, many of which are known to directly regulate virulence determinants (e.g. the Agr, Sae, and Arl systems) (Haag & Bagnoli, 2015; Jenul & Horswill, 2019). The *S. aureus* exoprotein expression (Sae) TCS is known to regulate virulence factors with functions such as adhesion, hemolysis, and proteolysis, (including *hla*, *hlgA/B/C*, *sspA*, *aur*, and *fnbA*) (Jenul & Horswill, 2019; Liu et al., 2016; Rogasch et al., 2006), through the use of two classes of target binding sites. Class I targets, also known as low-affinity targets, are known to be upregulated in strain Newman, which has increased basal levels of SaeS kinase activity, and includes genes such as *coa*, *eap*, *and sbi* (Liu et al., 2016; Rogasch et al., 2006). Class II targets, also known as high-affinity targets, are insensitive to changes in basal kinase activity and include genes such as *hla* (Jeong et al., 2012; Liu et al., 2016; Mainiero et al., 2010). The SaeRS system is activated by a range of stimuli, including calprotectin, hydrogen peroxide, and human neutrophil proteins 1–3, all of which play a role in the human immune response (Cho et al., 2015; Geiger et al., 2008). The ArlRS system has been established to regulate genes involved in a variety of cellular functions including *ebh* and *sdrD* (involved in adhesion), virulence factors such as *nuc*, *lukA*, *esxA*, and transcriptional regulators such as *sarV*, and *mgrA* (Crosby et al., 2020). The regulation of adhesins by ArlRS is critical to endovascular infection (Kwiecinski et al., 2019). One known signal for ArlRS activation is disruption of glycolysis, specifically through a reduction in manganese (Párraga Solórzano et al., 2019), suggesting that ArlRS may be activated in nutrient-poor environments.

Although two-component systems, and stand-alone regulators (such as the Sar family), have been the primary focus of gene regulation studies in *S. aureus*, recently, sRNAs have emerged as potent regulators of processes such as virulence, biofilm formation, and stress response (Bronesky et al., 2016; Lalaouna et al., 2019; Romilly et al., 2012). In addition to carrying out regulatory roles on their own, several sRNAs have also been shown to carry open reading frames encoding small peptides (Janzon et al., 1989; Nielsen et al., 2011), which can carry out functions independent of the sRNA. The best-studied example of this type of molecule in *S. aureus* is the delta toxin Hld, an α-type phenol soluble modulin (PSM), which is encoded on the sRNA RNAIII. While RNAIII coordinates the regulation of a variety of *S. aureus* virulence genes (as an RNA molecules), Hld also functions as a hemolysin. Small proteins/peptides are likely widespread in bacterial genomes but are not annotated due to their small size (Garai & Blanc-Potard, 2020; Miravet-Verde et al., 2019; Schilcher et al., 2020).

Previous work by our group generated updated *S. aureus* annotation files to include previously identified sRNA molecules (Carroll et al., 2016). In the same study, we identified 39 novel putative sRNAs, named tsr1-39, several of which demonstrated altered expression in human serum compared to TSB (Carroll et al., 2016). A number of the newly identified tsr transcripts had the potential to encode small proteins or peptides. Follow-up work by our group revealed that three of the tsr transcripts (tsr21, tsr22, and tsr37) encode small proteins (Sorensen et al., 2020). During this analysis, we observed that overexpression of a histidine tagged protein, encoded on the tsr37 transcript, led to a dramatic increase in cellular aggregation in the absence of human serum.

In this study, we investigate the biological role and function of the tsr37 encoded protein (herein renamed ScrA for Staphylococcal clumping regulator A). We show that ScrA contributes to *S. aureus* auto-aggregation, leading to increased clumping in planktonic cultures, and to increased biofilm formation. Whole-cell transcriptomics and mass spectrometry of secreted proteins revealed the expression of several virulence factors is altered upon ScrA overexpression, many of which are part of the SaeRS regulon. We go on to demonstrate that ScrA-mediated phenotypes require a functional SaeRS system, strongly suggesting that ScrA activates the Sae system. Finally, we demonstrate a role for the ArlRS TCS in activating expression of *scrA* and show that the SaeRS system has a negative influence on *scrA* expression. Based on these results we hypothesize that ScrA acts as an intermediary linking the ArlRS and SaeRS systems.

2 | RESULTS

2.1 | Investigation of the *scrA* locus

Previously, we demonstrated that overexpressing a 6x-his tagged version of the ScrA protein resulted in increased autoaggregation of *S. aureus* cells (Sorensen et al., 2020). The construct used in the previous study (pScrA-His) consisted of the ScrA open reading frame fused to six histidine residues, and an ~300 bp upstream region, leaving the protein under the control of its native promoter (Figure 1a). Since the *scrA* transcript was truncated in this construct, we constructed a second *scrA* overexpression plasmid containing the entire *scrA* gene, (pScrA), which also expressed *scrA* under control of its native promoter (but did not contain a his tag on the ScrA open reading frame) (Figure 1a). The MRSA252 and NCTC8325 genomes contain annotations for a gene immediately downstream of *scrA*, which is not annotated in USA300. Previously published data by Mäder et al. (2016) suggested that ScrA and the downstream gene (which we have designated *scrB*) are encoded on a polycistronic transcript (Figure 1b). To investigate if *scrB* contributes to the clumping phenotype observed, we constructed a third overexpression plasmid (pScrAB) containing both the *scrA* and *scrB* genes under control of their native promoter (s) (Figure 1a). To investigate the operon structure of *scrA* and *scrB*, a Northern blot was performed using RNA samples from wild-type *S. aureus* containing either pMK4 (empty vector control) or pScrAB. An *scrA* mutant (containing the empty vector pMK4) was included as a negative control. Using a probe that encompasses the 267 nt *scrA* open reading frame (Figure 1a, red bar) we detected an ~480 nt band in the wild type and ScrAB overexpressing strains (Figure 1c), while no bands were detected in the *scrA* mutant. We were unable

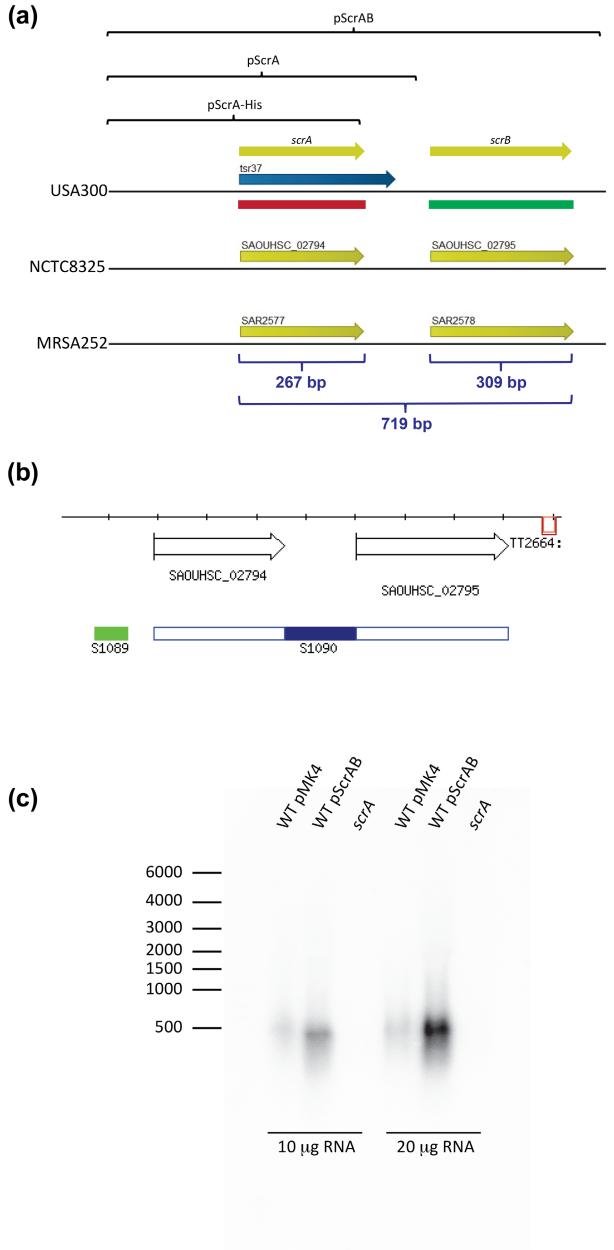

FIGURE 1 Predicted transcript architecture of the *scrAB* locus. (a) Three overexpression plasmids were constructed to express either a his tagged ScrA (pScrA-his), *scrA* (pScrA), or *scrA* and *scrB* (pScrAB). (b) Data previously published by Mäder et al. (2016) suggest that *scrAB* is encoded on a polycistronic transcript. (c) Northern blot of wild-type *S. aureus* containing the pMK4 empty vector (WT pMK4), wild-type *S. aureus* containing *pscrAB* (WT pScrAB), and the *scrA* mutant (*scrA*). Blots were probed with a riboprobe antisense to the *scrA* open reading frame. Blots were loaded with either 10 or 20 µg of total RNA as indicated. Red bar in panel a indicates the sequence used to generate the *scrA* northern probe, while the *scrB* probe sequence in indicated by a green bar

to detect any *scrB* transcript when probing 20 µg of total RNA with a 309 nt *scrB*-specific probe (data not shown). No band corresponding in size to polycistronic *scrAB* transcript was detected. The size of the *scrA* transcript detected (~480 nt) is consistent with a transcript encompassing the *scrA* coding sequence (267 nt) plus approx. 200 nt of untranslated sequence, strongly suggesting that *scrA* is monocistronic. Nonetheless, we cannot rule out the possibility that the *scrA* transcript detected arose as a result of processing a longer *scrAB* transcript.

2.2 | ScrA-induced clumping is not strain specific and leads to aggregation in both planktonic and static cultures

During our initial investigation into ScrA function, bacterial cells were observed to spontaneously clump in the absence of human serum, a phenotype that can be quantified by measuring OD_{600} before and after static incubation (Sorensen et al., 2020). To investigate if this clumping was specifically due to *scrA* overexpression, or an artifact resulting from overexpressing a truncated form of *scrA*, we subjected strains containing the three overexpression constructs (pScrA-his, pScrA, and pScrAB), to a clumping assay in the absence of human serum. OD_{600} was determined before and after incubation, and all three *scrA* overexpression strains showed an increase in clumping over the pMK4 empty vector control. The pScrA-his containing strain demonstrated ~40% clumping after a 2 h incubation, while pScrA and pScrAB containing strains showed ~80% clumping (Figure 2a). The similarity in clumping between pScrA and pScrAB strains, and the absence of *scrB* in the pScrA plasmid, indicates that ScrA is primarily responsible for the observed clumping phenotype.

Due to the presence of ScrA and ScrB homologs in MRSA252 and NCTC8325, we next sought to determine if ScrA function was restricted to AH1263 or extended to additional *S. aureus* backgrounds. To investigate this, we introduced the pScrAB overexpression plasmid into the *S. aureus* backgrounds SH1000, Newman, and UAMS-1, along with the empty vector control pMK4. While the background rate of clumping varied by strain, an increase in clumping was observed when overexpressing pScrAB, in all *S. aureus* backgrounds tested (Figure 2b), demonstrating that the ScrA clumping phenotype is not limited to the *S. aureus* USA300 lineage (AH1263).

Our initial assay using pScrA and pScrAB suggests that ScrA is responsible for clumping. To confirm this hypothesis, and determine the role of each gene (*scrA* and *scrB*) in clumping, we utilized the cadmium-inducible promoter in plasmid pCN51, to overexpress either *scrA* alone, *scrB alone*, or both *scrA* and *scrB*. Wild-type *S. aureus* containing the pCN51 plasmids were subjected to a clumping assay after overnight growth with 10 µM cadmium chloride to induce expression. When compared with the pCN51 empty vector control, pCN51_ScrAB demonstrated ~80% clumping, similar to levels observed when under control of the native *scrA* promoter on pMK4 (Figure 2c). Similar levels of clumping were observed using the pScrA construct (~80% clumping). In contrast, strains containing the pScrB construct demonstrated no significant difference compared to the empty vector control (Figure 2c). These results clearly demonstrate that ScrA is solely responsible for the observed clumping phenotype. However, since the operon

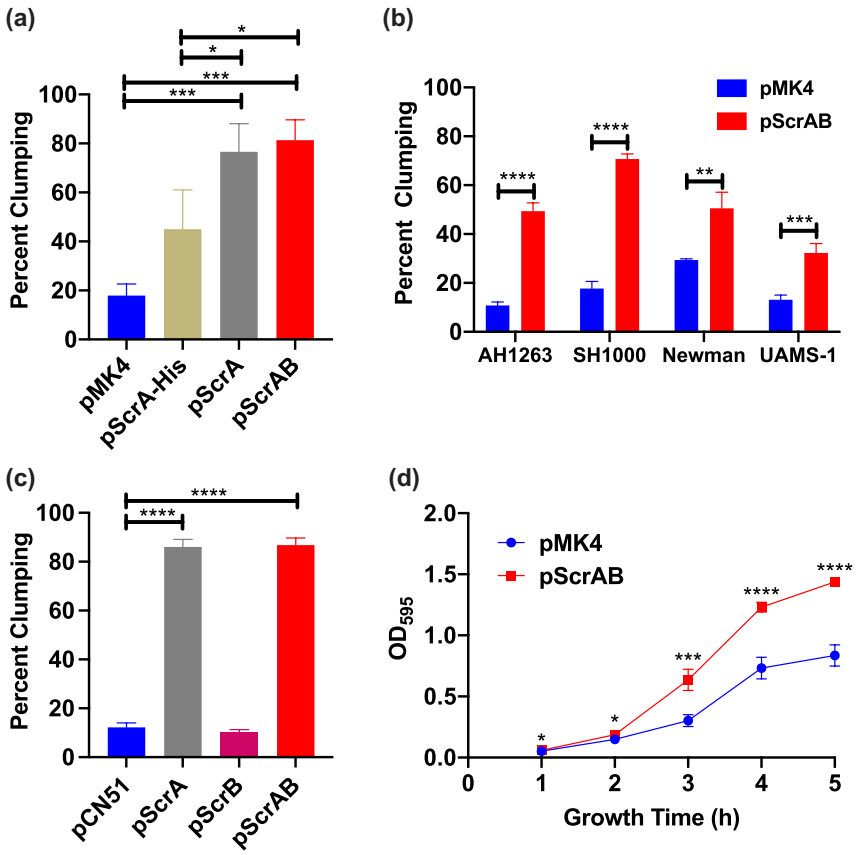

FIGURE 2 Overexpression of *scrA* induces clumping. (a) *S. aureus* containing the pMK4 empty vector as well as the three overexpression constructs were grown overnight and were left static for 2 h. The initial and final OD_{600} of the top 100 µl were used to calculate clumping. (b) The *scrAB* overexpression plasmid was transduced into *S. aureus* strains SH1000, Newman, and UAMS-1, and clumping was assessed. An increase in clumping was observed in each background. (c) Individual overexpression of either *scrA*, *scrB*, or scrAB was performed in plasmid pCN51 to determine the contribution of each individual transcript to clumping. Overexpression was driven by a cadmium-inducible promoter. Increased clumping was only observable when overexpressing *scrA*. (d) A biofilm formation assay was performed over time with wild-type *S. aureus* containing the pMK4 empty vector (pMK4) and the *scrAB* overexpressing strain (pScrAB). A statistically significant increase in biofilm formation was observed in the *scrAB* overexpressing strain. Experiments were performed for a minimum of three times for panels a, b, c, and d, respectively. Error bars represent standard deviation. Statistical significance was determined using an ordinary one-way ANOVA and Tukey's multiple comparison for panels a–c. Student's *t*-test was used at each time point for panel d; $^{*}p < 0.05$, $^{**}p < 0.01$, $^{***}p < 0.005$, $^{****}p < 0.001$

structure of *scrAB* is unclear, to ensure optimal production of ScrA all further experiments were performed with the pScrAB construct under control of its native promoter as our primary overexpressor plasmid.

It is well established that interactions between bacterial surface proteins can mediate the initial phases of biofilm formation (Jin et al., 2019). To investigate if the clumping phenotype observed in planktonic cultures overexpressing ScrA influences biofilm formation, we used our ScrA overexpressing strain in a biofilm assay. Experiments were performed in 24-well plates coated with human serum and inoculated with either the empty vector control or ScrA overexpressing strain. The wells were washed at 1 h intervals (from 1 to 5 h), and biofilm quantity was determined by crystal violet retention. Results show that the ScrA overexpressing strain developed more robust biofilms when compared with the empty vector control (Figure 2d). This suggests that ScrA overexpression induces clumping not only to other bacterial cells (as is likely in planktonic cultures), but also induces adhesion to host serum proteins.

2.3 | ScrA-mediated clumping is due to an encoded small protein

While the *scrA* gene was observed to influence clumping, it was unclear if the effector was the *scrA* transcript itself acting as a small RNA, or the small protein encoded within. To determine which molecule is the effector, we constructed 2 *scrA* expression plasmids containing nonsense mutants. A TAA stop codon was introduced into the pCN51_ScrA overexpression plasmid at either the 3rd (pCN51_ScrA_NSAA3) or 8th (pCN51_ScrA_NSAA8) codon, and expression induced by the addition of cadmium chloride. In a clumping assay, neither nonsense mutant was observed to have increased clumping (Figure 3a), suggesting that the observed clumping phenotype is due

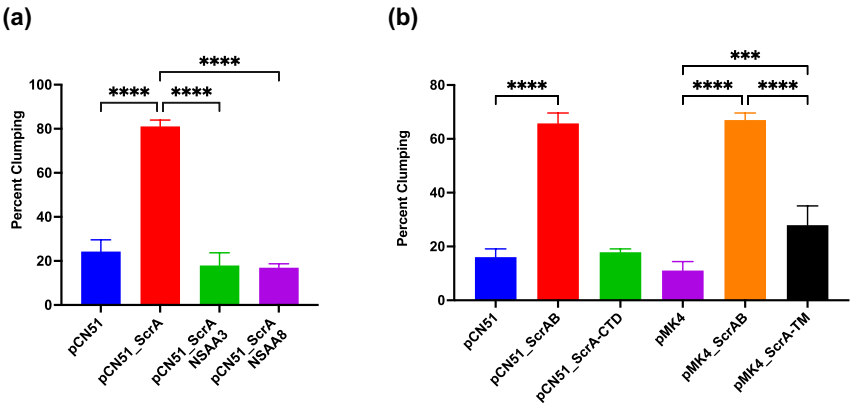

FIGURE 3 Role of the ScrA protein in clumping. (a) Serum-free clumping assay performed using *S. aureus* containing the empty vector (pCN51), overexpressing native ScrA (pCN51_ScrA), overexpressing ScrA with a nonsense mutation at amino acid 3 (pCN51_ScrA_NSAA3), or overexpressing ScrA with a nonsense mutation at amino acid 8 (pCN51_ScrA_NSAA8). (b) Serum-free clumping assay performed on *S. aureus* containing either the empty vector (pCN51, pMK4), overexpressing full-length *scrA* (pCN51_ScrAB, pMK4_ScrAB), overexpressing the ScrA C-terminal tail (pCN51_ScrA-CTD), or overexpressing the ScrA transmembrane domain (pMK4_ScrA-TM). Experiments were performed for a minimum of three times. Error bars represent standard deviation. Statistical significance was determined using an ordinary one-way ANOVA and Tukey's multiple comparison. $^{*}p<0.05$, $^{**}p<0.01$, $^{***}p<0.005$, $^{****}p<0.001$

to the encoded ScrA protein. Expression of *scrA* was confirmed to be similar between the nonsense mutants and native sequence by RT-qPCR (data not shown).

Computer modeling of ScrA predicts 2 distinct domains, a transmembrane helix, and a C-terminal domain. To determine which domains are responsible for clumping, we overexpressed a truncated ScrA consisting of only the transmembrane domain driven by its native promoter in pMK4. Additionally, we constructed a plasmid overexpressing the ScrA C-terminal domain driven by a cadmium-inducible promoter in pCN51. Clumping assays showed a modest increase in clumping when the transmembrane domain alone was expressed, although the level of clumping observed was significantly lower than that observed when overexpressing the full-length protein (Figure 3b). Overexpression of the C-terminal domain alone did not result in increased clumping. Together, these data suggest that the clumping phenotype observed is mediated by a protein encoded by the *scrA* gene in which the transmembrane domain is essential to its function.

2.4 | ScrA influences *saeRS* abundance and secreted virulence factors

Overexpression of ScrA leads to increases in clumping and biofilm formation, however, the exact mechanism underlying these processes remains unclear. The clumping phenotype could be mediated directly by ScrA, however, we deemed this unlikely due to the small size of the ScrA protein and it's predicted localization in the cell membrane. Alternatively, ScrA could mediate clumping indirectly via some additional *S. aureus* factor (s). To investigate how ScrA influences clumping we first performed whole transcriptomics by RNA sequencing (RNA-seq) to determine how ScrA overexpression alters the bacterial transcriptome (compared to empty vector control). Strains were grown to mid-exponential phase, RNA extracted, and RNA-seq performed. Raw data were analyzed and visualized by volcano plot (Figure 4a, Table S1). To identify genes significantly altered upon ScrA expression, a differential expression analysis was performed using the following parameters; 2-fold change in expression, a $p<0.05$, and a mean reads per kilobase of transcript per million mapped reads (RPKM) >10 in either strain (Figure 4a, red dots). In total, 353 genes were altered with 151 upregulated upon ScrA overexpression and 201 downregulated. The 10 most upregulated and 10 most downregulated genes (by abundance) are listed in (Figure 4b). The two most highly upregulated protein coding genes were the surface adhesins *coa* and *empbp* at 25.5- and 25.4-fold upregulated, respectively. The *map* gene, encoding the secreted adhesin Map was also highly upregulated (20.5-fold). Upregulation of these genes could explain the increase in biofilm formation observed (Figure 2d), as their gene products encode proteins capable of binding host factors. Interestingly *saeS* which encodes the sensor kinase of the SaeRS two-component system, was upregulated 7.76-fold. The response regulator *saeR* was also found to be upregulated (7.18-fold), while the *saeP* (SAUSA300_0692) and *saeQ* (SAUSA300_0693) genes were upregulated 3.32- and 5.77-fold, respectively (Table S1). SaeRS is known to positively autoregulate its own expression (Liu et al., 2016), suggesting that overexpression of ScrA may lead to SaeRS activation. To confirm and validate the RNA-seq data, we performed RT-qPCR on two genes shown to be upregulated upon ScrA overexpression (i.e., *coa* and *saeS*). Results confirmed the RNA-seq data showing that both genes were upregulated in the ScrAB overexpression strain, (Figure S1).

The SaeRS system is a global regulator of secreted virulence factors in *S. aureus* (Giraudo et al., 1997; Liu et al., 2016; Mainiero et al., 2010), therefore we next investigated changes to the *S. aureus* secreted protein profile (secretome) upon ScrA overexpression. Overnight cultures (*scrA* overexpressor and empty vector control)

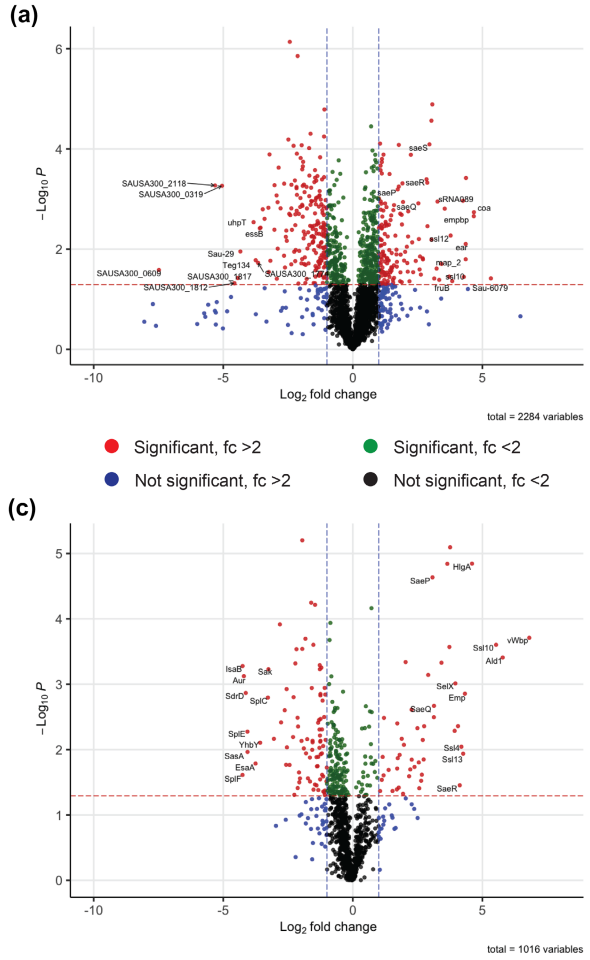

(b)

Gene	Gene number	Description	Fold Change
Sau-6079	SAUSA300s182	Small RNA (sRNA)	40.2
coa	SAUSA300_0224	Staphylocoagulase	25.5
empbp	SAUSA300_0774	Extracellular matrix protein-binding protein	25.4
ssr8	SAUSA300s117	Small RNA (sRNA)	20.6
map_2	SAUSA300_1917	Map protein	20.5
ear	SAUSA300_0815	Ear Protein	20.5
ssl10	SAUSA300_0398	Staphylococcal superantigen like protein	19.5
sRNA089	SAUSA300s214	Small RNA (sRNA)	19.1
fruB	SAUSA300_0684	Fructose 1-phosphate kinase	14.3
ssl12	SAUSA300_1059	Staphylococcal superantigen like protein	13.7
essB	SAUSA300_0282	Type VII secretion system protein	-12.1
SAUSA300_1774	SAUSA300_1774	tRNA-Asn	-12.6
Teg134	SAUSA300s151	Small RNA (sRNA)	-13.4
uhpT	SAUSA300_0216	Hexose phosphate transport protein	-14.2
Sau-29	SAUSA300s177	Small RNA (sRNA)	-20.3
SAUSA300_1817	SAUSA300_1817	tRNA-Trp	-21.7
SAUSA300_1812	SAUSA300_1812	tRNA-Pseudo	-23.7
SAUSA300_0319	SAUSA300_0319	Putative membrane protein	-33.1
SAUSA300_2118	SAUSA300_2118	tRNA-Tyr	-39.9
SAUSA300_0609	SAUSA300_0609	Phage integrase family protein	-179.1

(d)

Protein	Gene number	Description	Fold Change
vWbp	SAUSA300_0773	Von Willebrand binding protein	112.1
Ald1	SAUSA300_1331	Alanine dehydrogenase	55.1
Ssl10	SAUSA300_0398	Superantigen like protein	46.1
HlgA	SAUSA300_2365	Gamma-hemolysin component A	24.2
Emp	SAUSA300_0774	Extracellular matrix protein-binding protein	20.0
Ssl13	SAUSA300_1060	Superantigen like protein	19.1
Ssl4	SAUSA300_0404	Superantigen like protein	18.2
SaeR	SAUSA300_0691	Response Regulator	17.5
Ssl12	SAUSA300_0396	Superantigen like protein	16.7
SelX	SAUSA300_0370	Staphylococcal enterotoxin-like toxin X	15.5
Sak	SAUSA300_1922	Staphylokinase	-9.6
SplC	SAUSA300_1756	Serine protease	-9.7
YhbY	SAUSA300_1554	Predicted RNA-binding protein	-11.9
EsaA	SAUSA300_0279	Type VII secretion system accessory factor	-13.5
SasA	SAUSA300_2581	Putative surface anchored protein	-16.7
SplE	SAUSA300_1754	Serine protease	-16.8
SdrD	SAUSA300_0547	Serine-aspartate repeat-containing protein D	-17.5
Aur	SAUSA300_2572	Zinc metalloproteinase aureolysin	-18.4
IsaB	SAUSA300_2573	Immunodominant staphylococcal antigen B	-19.1
SplF	SAUSA300_1753	Serine protease	-19.1

FIGURE 4 Transcriptomic and proteomic analysis of ScrA overexpressing strain. (a) RNA sequencing was performed on 3 h cultures of *S. aureus* containing the pMK4 empty vector and the *scrAB* overexpressing strain. Differential expression analysis was performed, and the results were visualized on a volcano plot. Significance was determined using Student's *t*-test. Log_2 fold change is shown on the x axis, while $-\log_{10} p$ is shown on the y axis. Genes indicted by red circles displayed a fold change >2 and p value was <0.05. (b) The 10 genes demonstrating the highest fold increase and decrease in expression in the *scrAB* overexpressing strain. Several adhesions, including *coa*, *empbp*, and *sbi*, were identified as being upregulated in a *scrAB* overexpresser. (c) The secreted protein profiles of *S. aureus* containing the pMK4 empty vector and the *scrAB* overexpressing strain were analyzed by mass spectrometry proteomics. Differential expression analysis was performed, and the results were visualized on a volcano plot. Significance was determined using Student's *t*-test. Log_2 fold change is shown on the x axis, while $-\log_{10} p$ is shown on the y axis. Genes indicated by red circles displayed a fold change >2 and *p* value was <0.05. (d) the 10 proteins demonstrating the highest fold increase and decrease in abundance in the *scrAB* overexpressing strain

were pelleted via centrifugation and the supernatants were TCA precipitated to concentrate proteins. Liquid chromatography coupled to mass spectrometry was utilized to identify proteins and determine their abundance. Data were visualized by volcano plot (Figure 4c) and differential expression analysis was performed using similar criteria as those employed for RNAseq (2-fold change in expression, a $p < 0.05$) (Table S2). 135 proteins were altered with 50 upregulated upon ScrA overexpression and 85 downregulated. The 10 most upregulated and 10 most downregulated proteins by abundance are listed in Figure 4d. Notably, the Von Willebrand binding protein (vWbp) and extracellular matrix binding protein (Empbp) were 112-fold and 20-fold upregulated, respectively, while numerous superantigen-like proteins were also increased upon ScrA overexpression (Figure 4c,d). Proteases SplF, Aur, SplE, and SplC were downregulated. Another target of SaeRS, gamma hemolysin component A (HlgA) was found to be 24-fold upregulated, while gamma hemolysin component B (HlgB) was 7.5-fold upregulated. Collectively, these data are broadly consistent with both SaeRS activation, and the observed clumping and biofilm phenotypes observed in an ScrA overexpresser.

2.5 | ScrA overexpression leads to an increase in HlgA-mediated hemolysis

As noted above, increases in HlgA and HlgB proteins were observed upon *scrA* overexpression. HlgA and HlgB form a heterodimer, which is capable of lysing human erythrocytes. Therefore, to determine if changes in HlgAB levels were biologically significant we examined the consequence of *scrA* overexpression on the hemolytic activity of

S. aureus. Human erythrocyte lysis assays were performed using the ScrA overexpressing strain and empty vector control. Results show an approx. 7-fold increase in hemolytic activity in the ScrA overexpressing strain compared to the empty vector control (Figure 5). The αPSMs are toxic peptides produced by *S. aureus* and are potent cytotoxins, particularly against human erythrocytes (Giraudo et al., 1997; Wang et al., 2007; Zapf et al., 2019). No difference in αPSM levels was observed in the secretomic analysis, suggesting that the differences observed in hemolysis are HlgAB mediated. This result supports the proteomic data and suggests that the increase in gamma hemolysin production observed in the ScrA overexpressing strain manifests as a biologically meaningful increase in activity.

2.6 | SaeRS is essential for ScrA function

The phenotypes observed above (Figure 2) and transcriptomic/proteomic data (Figure 4) strongly suggest the SaeRS system is activated in response to ScrA overexpression. To determine if SaeRS is essential for the observed ScrA-mediated phenotypes, we overexpressed ScrA in *saeR* and *saeS* mutant backgrounds and examined clumping of each strain compared to empty vector controls. As previously observed, overexpression of ScrA led to increased clumping in the wild-type background, however, overexpression of ScrA did not lead to any measurable increase in clumping in either the *saeR* or *saeS* mutant strains (Figure 6a), indicating that ScrA-mediated clumping requires both SaeR and SaeS. We next investigated the requirement for SaeRS in ScrA-mediated biofilm formation. A biofilm assay was performed using wild-type *S. aureus* (AH1263) and the *saeR* mutant, containing either the empty vector or ScrA overexpression plasmid (Figure 6b). As previously observed, ScrA overexpression in the wild-type background led to a more robust biofilm, while ScrA overexpression in an *saeR* mutant showed no increase over the empty vector control. These results strongly suggest that ScrA is functioning via the SaeRS system, either directly or indirectly. To confirm that the abrogation of ScrA-mediated phenotypes in *sae* system mutants is specifically due to the inactivation of the SaeRS system, we overexpressed ScrA in an *agrA* mutant (AgrA is the response regulator of the Agr two-component system). ScrA overexpression in the *agrA* background led to an increase in clumping similar to that observed in the wild-type background (Figure S2), confirming that ScrA-mediated phenotypes specifically require an intact SaeRS system.

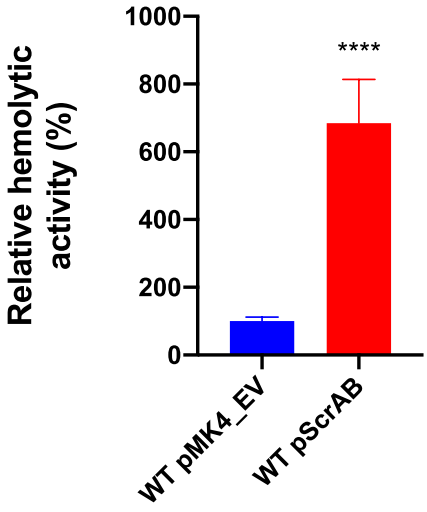

FIGURE 5 ScrAB overexpressing leads to increased hemolytic activity against human erythrocytes. Cultures of *S. aureus* containing the pMK4 empty vector (WT pMK4_EV) and the *scrAB* overexpressing strain (WT pScrAB) were grown for 15 h and hemolysis assays were performed with cell-free culture supernatants. An ~7 fold increase in hemolytic activity was observed in the *scrAB* overexpressing strain compared to the empty vector control. Experiments were performed four times. Error bars represent standard deviation. Significance was determined using Student's *t*-test $^{*}p<0.05$, $^{**}p<0.01$, $^{***}p<0.005$, $^{****}p<0.001$

2.7 | ScrA expression is positively regulated by ArlR and negatively regulated by SaeR

Previous work by Rapun-Araiz et al. (2020), overexpressed individual two-component system (TCS) response regulators and used RNA-seq to investigate the specific regulons and direct targets of each TCS in *S. aureus*. We re-examined the data generated in this study to determine expression values (in each TCS overexpressing strain) for *scrA*, which was absent from the USA300 genome file used as a reference in the study. To generate values for *scrA* we utilized an updated USA300 reference genome, previously generated by our group, that contains annotations for sRNA genes (*scrA* was originally annotated as tsr37/SAUSA300s301 in this study; Carroll et al., 2016; Sorensen et al., 2020. The goal of this analysis was to determine if *scrA* expression was under the control of any TCS in *S. aureus*. Results show that for 15 of the 16 TCS in *S. aureus* there was no significant variation in *scrA* expression when a constitutively active form of the response regulator was expressed (Figure 7a). However, a 25-fold increase in *scrA* expression was observed when the ArlR response regulator was overexpressed (Figure 7a). These data strongly suggest that *scrA* is positively regulated by the ArlRS TCS.

To further explore the Arl-ScrA-Sae regulatory pathway, and confirm that ArlR positively regulates *scrA*, we performed RT-qPCR to examine *scrA* transcript levels following 3-, 6-, and 9- h of growth in TSB. RNA for RT-qPCR was isolated from WT *S. aureus* and an *arlR* mutant containing the ScrA overexpression plasmid (in which *scrA* is under the control of its native promoter). We also included the *saeR* mutant (containing the ScrA overexpression plasmid) in the analysis to investigate if SaeR was downstream of ScrA in the regulatory pathway. At 3 h *scrA* expression was reduced in the *arlR* mutant ~3-fold relative to the wild type (Figure 7b), which is consistent with ArlR positively regulating *scrA*. This reduction was also observed at 6 h, although the effect was slightly less that 2-fold, and by 9 h no significant difference was observed (Figure 7b). Surprisingly, *scrA* expression in the *saeR* mutant, was increased ~3.5-fold at 6 and 9 h. This increase is suggestive of a negative feedback loop by SaeR on *scrA* expression and the absence of SaeR leads to derepression and

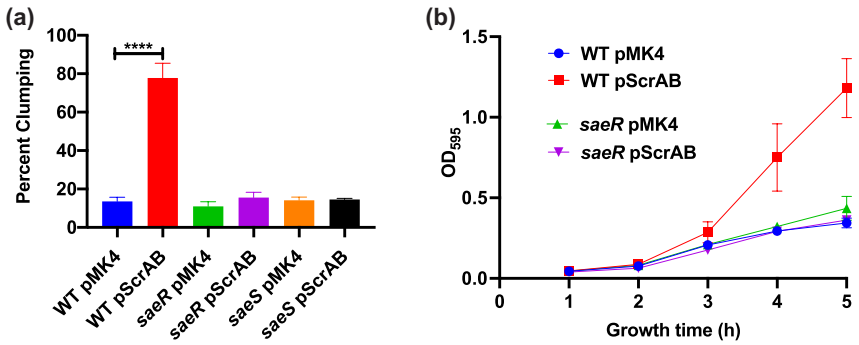

FIGURE 6 The SaeRS system is required for ScrA-mediated phenotypes. (a) Clumping assays were performed in wild-type *S. aureus*, *saeR*, and *saeS* mutants overexpressing *scrAB*. No increase in clumping was observed when either *saeR* or *saeS* was disrupted. (b) Biofilm assays were performed in wild-type *S. aureus* and an *saeR* mutant overexpressing *scrAB*. No increase in biofilm formation was observed when ScrA was overexpressed in the *saeR* mutant. Experiments were performed four times. Error bars represent standard deviation. Significance was determined using a standard one-way ANOVA and Tukey's multiple comparison. $^{*}p < 0.05$, $^{**}p < 0.01$, $^{***}p < 0.005$, $^{****}p < 0.001$

(a)

scrA expression (SAUSA300s301)

TCS	Fold Change	Mutant mean	Overexpressor mean
AgrA	-1.08	40.62	37.69
AirR	1.3	41.53	53.8
ArlR	25.77	42.87	1,104.59
BraR	1.54	40.8	62.86
GraR	-1.19	43.2	36.31
HtpR	-1.17	42.3	36.3
HssR	-1.26	39.85	31.63
KdpE	1.05	39.49	41.59
LytR	1.26	45.26	56.99
NreC	-1.05	39.36	37.5
PhoP	-2.12	38.23	17.99
SaeR	1.19	42.88	51.23
SsrA	-1.18	41.46	35.09
TCS7	-1.2	42.77	35.66
VraR	1.11	41.64	46.4
WalR	-1.13	39.36	34.72

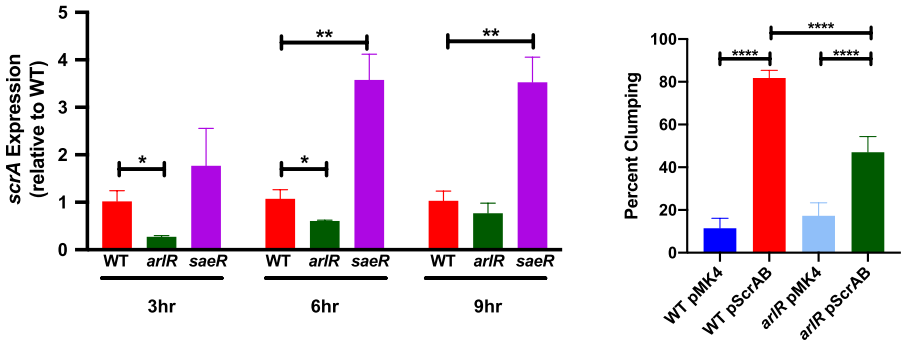

FIGURE 7 ArlR positively regulates *scrA* expression. (a) Reanalysis of data previously published by Rapun-Araiz et al. (2020) demonstrated that constitutive expression of ArlR resulted in an approx. 25-fold increase in *scrA* expression. No other TCS response regulator increased *scrA* expression when constitutively activated. (b) Quantification of *scrA* transcript abundance in *S. aureus* WT, *arlR*, and *saeR* mutant strains containing the *scrAB* overexpression plasmid following 3, 6, and 9 h growth. Abundance of *scrA* transcript in each strain was determined by RT-qPCR and normalized against the value in the WT strain at each timepoint. A significant decrease in *scrA* expression was observed in the *arlR* mutant at both 3 and 6 h, but there was no significant difference by 9 h. Interestingly disruption of *saeR* resulted in increased *scrA* expression at 3, 6, and 9 h of growth. (c) Clumping assays were performed using WT *S. aureus* and the *arlR* mutant containing the *scrAB* overexpression plasmid. Overexpressing *scrAB* in the *arlR* mutant led to a significant increase in clumping, but not to the same extent observed in the WT strain. The increase in clumping in the *arlR* mutant was significantly lower than that in the WT background. Experiments were performed four times. Error bars represent standard deviation. Significance was determined using a Student's *t*-test for panel B and an ordinary one-way ANOVA and Tukey's multiple comparison for panel C. $^{*}p < 0.05$, $^{**}p < 0.01$, $^{***}p < 0.005$, $^{****}p < 0.001$

increased transcription of *scrA*. Analysis of the promoter region of *scrA* showed no canonical SaeR-binding site, suggesting that either SaeR is binding to an alternative sequence or that Sae-mediated repression of *scrA* is indirect and facilitated by a downstream target of SaeR.

Finally, since ArlR positively influences ScrA expression, we sought to determine if the absence of *arlR* leads to decreased ScrA activity. To investigate this, we overexpressed ScrA (or the empty vector) in wild-type AH1263, and the *arlR* mutant and subjected the strains to a clumping assay (Figure 7c). We observed an ~80% increase in clumping when ScrA was overexpressed in the wild-type strain, consistent with previous assays. In the *arlR* mutant background, an increase in clumping was observed, however, the increase was less than that observed in the WT (~50% increase in clumping). This further suggests a positive regulatory role of ArlR on *scrA*. However, the increase in clumping also suggests that *scrA* expression is not entirely dependent on *arlR* and additional unidentified regulators of *scrA* expression may exist in the cell. This is consistent with the RT-qPCR data taken at 9 h (Figure 7b).

2.8 | ScrA overexpression leads to increased Sae-dependent membrane stability

The ScrA protein is 88 amino acids in length and contains one predicted transmembrane helix. Overexpression of a protein containing a transmembrane helix, such as ScrA, and subsequent insertion of the protein into the cell membrane, could potentially destabilize

the membrane, and therefore, while unlikely, it is possible that this nonspecific membrane destabilization could cause all of the phenotypes outlined in this study. To investigate if the ScrA-mediated phenotypes observed in this study are due to alterations in membrane stability (as a result of increased accumulation of ScrA in the membrane), we examined membrane integrity using the nonmembrane permeable dye propidium iodide, which is fluorescent when it enters through damaged membranes and intercalates into DNA. Cells were harvested by centrifugation, washed, and incubated with propidium iodide. Overexpression of ScrA in WT *S. aureus* led to increased permeability of the membrane suggesting some alterations in membrane stability arise from ScrA overexpression (Figure 8). However, when ScrA was overexpressed in the *saeR* mutant, no increase in permeability was observed. This result indicates that the increase in membrane instability is not directly attributable to the production of ScrA (which is high in the *saeR* mutant, Figure 7b), but rather it is a result of the activation of the SaeRS system that accompanies ScrA overexpression. Consistent with this, an increase in membrane instability was also observed, albeit to a lesser degree, in the *arlR* mutant. This result mirrors the results from the clumping assay (Figure 7c) again suggesting that membrane instability is not due to ScrA per se, but is instead due to the function of downstream targets, affected by ScrA overexpression.

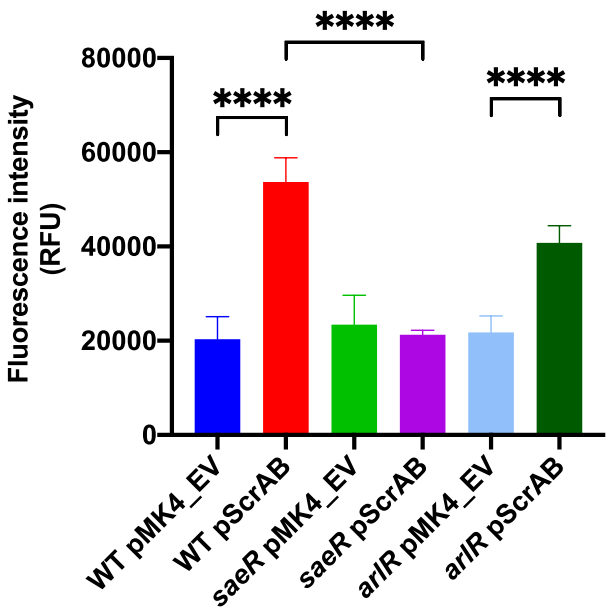

FIGURE 8 Overexpression of *scrAB* leads to membrane instability in an SaeRS-dependent manner. Propidium iodide staining was used to measure membrane stability. Increased fluorescence is indicative of greater instability. Overexpression of *scrAB* in the wild-type strain resulted in a significant decrease in membrane stability, while no difference in membrane stability was observed following *scrAB* overexpression in the *saeR* mutant strain. Membrane instability was also increased following *scrAB* overexpression in the *arlR* mutant although not to the same degree as in WT *S. aureus*. Error bars represent standard deviation. Significance was determined using an ordinary one-way ANOVA and Tukey's multiple comparison. $^{*}p<0.05$, $^{**}p<0.01$, $^{***}p<0.005$, $^{****}p<0.001$

3 | DISCUSSION

In this study, we demonstrate that overexpression of the ScrAB locus results in changes to the global expression of adhesins, proteases, hemolysins, and the two-component system SaeRS. Observed changes in the transcriptome and secretome are consistent with, and suggestive of, overstimulation of the SaeRS system. ScrAB-mediated phenotypes are dependent on the presence of an intact SaeRS system, with observed clumping, biofilm, and hemolysis phenotypes abrogated when *saeR* or *saeS* was disrupted by a transposon insertion (Figure 6). Much of our understanding of the SaeRS regulon comes from *S. aureus* strain Newman, which shows increased basal kinase activity due to an L18P mutation (Rogasch et al., 2006). Several genes known to be altered in strain Newman, [including *saeS*, *saeR*, *efb*, *embpb*, *splC*, *sbi*, *aur*, *sspA*, *hlgA*, and *hlgB* (Rogasch et al., 2006)), were also altered in our transcriptomic and secretomic data (Figure 4) strongly suggesting that the SaeRS system is being stimulated. Changes in HlgA were demonstrated to be biologically significant, as overexpression of pScrAB led to an ~7-fold increase in hemolytic activity (Figure 5). In addition to showing that ScrA promotes the SaeRS system, we have demonstrated that ArlR positively regulates *scrA* expression (Figure 7). Disruption of the ArlRS system resulted in a significant decrease in *scrA* expression. While it is possible that ArlR directly activates *scrA* expression, ArlR is also known to function indirectly through the global regulator MgrA. Activity of the *scrA* promoter may be mediated by direct binding of ArlR, or through binding by MgrA. We are currently investigating the molecular mechanism through which the ArlRS system influences *scrA* expression and in turn how this impacts the SaeRS system.

While it appears that ScrA acts through SaeRS, the exact mechanism of action of ScrA activity remains unclear. The SaeRS system is complex, being comprised of four proteins, SaePQRS. SaeR and SaeS are the response regulator and histidine kinase, respectively, while SaeP and SaeQ are accessory factors that modulate the phosphatase activity of SaeS (Jeong et al., 2012). ScrA may act by stimulating the kinase activity of SaeS, or alternatively, it could repress phosphatase activity, by inhibiting SaePQ function on SaeS. If ScrA acts directly to stimulate SaeS kinase activity then it may function in a manner similar to Human Neutrophil peptide 1 (HNP-1), which is known to activate SaeS kinase activity (Geiger et al., 2008). Furthermore, as previously mentioned, a point mutation (L18P) found in a transmembrane helix of SaeS in strain Newman has been shown to increase basal kinase activity of SaeS (Adhikari & Novick, 2008; Liu et al., 2016). It is tempting to speculate that interaction with this transmembrane helix by the intramembrane portion of ScrA, may alter the conformation of the helix in a manner similar to the L18P mutation, thus increasing kinase activity. RT-qPCR suggests that the SaeRS system has a negative feedback loop on *scrA* expression. This could serve as a circuit breaker and prevent over-activation of the

Sae system by ScrA and/or the ArlRS system. While it is possible that SaeR is directly mediating this repression, the lack of a canonical SaeR binding site suggests that negative feedback is indirect, mediated by a downstream target of SaeR. Interestingly, SaeR was not indicated as a repressor of *scrA* in our analysis of the reconstructed TCS data by Rapun-Araiz et al. (2020). This may be due to the low basal level of *scrA* expression and the absence of the activator ArlR in the SaeR overexpressing strain (the background strain for the experiments lacked all TCS response regulators other than the specific one being overexpressed). Thus, it is likely that the basal level of *scrA* transcription was low enough that additional repression would not lead to detectable changes in expression.

Throughout this study, we utilized an *scrAB* overexpressing plasmid, and while we have demonstrated that the phenotypes observed appear to be ScrA-dependent, we acknowledge the exact contribution of ScrA and ScrB to each phenotype is unclear. We have demonstrated that clumping is influenced by ScrA exclusively. However, the role of each protein in additional ScrA-mediated phenotypes (e.g. hemolysis, biofilm formation, Sae activation) was not investigated. While we consider it likely that ScrA is the primary factor responsible for these phenotypes further work is necessary to conclusively eliminate any contribution from ScrB in regulation of *S. aureus* virulence factor expression. Furthermore, the biological significance of these ScrAB-mediated phenotypic changes to the *S. aureus* cell and *S. aureus* pathogenesis requires further study. It has been established that *S. aureus* binding to Von Willebrand Factor (VWF), (mediated by vWbp), facilitates adherence to blood vessel walls and influences the establishment of endocarditis (Claes et al., 2017; Liesenborghs et al., 2019). Identification of vWbp being 112-fold upregulated in the ScrA overexpression strain (Figure 4d), suggests that ScrA may play a role in endocarditis. Experiments are ongoing in our laboratory to determine the contribution of ScrA to *S. aureus* infection.

This study has demonstrated that overexpression of the *scrAB* locus leads to SaeRS activation and substantial changes in both the transcriptome and secretome. These changes lead to alterations in cellular clumping, biofilm formation, and hemolytic activity against human erythrocytes. RT-qPCR revealed a positive regulatory role of ArlR on *scrA* expression, while SaeR appears to repress *scrA* expression. Collectively, these observations led us to hypothesize a working model whereby ScrA is acting as an intermediary between the ArlR and SaeRS systems (Figure 9). We hypothesize that activation of the ArlRS system, leads to increased expression of *scrA* by the ArlR response regulator (or indirectly through another regulator such as MgrA). ScrA then acts, either directly or through an unknown intermediary, on the Sae system, stimulating SaeS kinase activity. This activation leads to changes in the SaeRS regulon, including activating adhesins and hemolysins while repressing proteases, resulting in increased cellular aggregation, biofilm formation, and hemolysis. Following activation, SaeRS acts to repress *scrA* either directly or indirectly. This function of ScrA may represent a previously unidentified functional link between the ArlRS and SaeRS two-component systems in *S. aureus*.

4 | MATERIALS AND METHODS

4.1 | Strains and strain construction

All bacterial strains and plasmids used in this study are listed in Table 1. All oligonucleotides used are listed in Table 2. Transposon mutants were acquired from the Network on Antimicrobial Resistance in *Staphylococcus aureus* (NARSA) (Fey et al., 2013) and transduced into USA300 AH1263. Phage transduction of both transposon mutations as well as plasmids utilized bacteriophage Φ11. Transposon presence was confirmed for *agrB*, *arlR*, and *saeR*, via PCR utilizing primer pairs #0049/#0052, #0055/#0056, and #0057/#0058, respectively. Construction of overexpression plasmids utilized USA300 AH1263 genomic DNA as a template to amplify fragments for insertion as follows. Primer pair #0831/#0902 was used to generate a fragment used in the construction of pRKC0751, #0832/#0902 generated a fragment for the construction of the pRKC0752 plasmid. Primers #1045/#1046 generated a

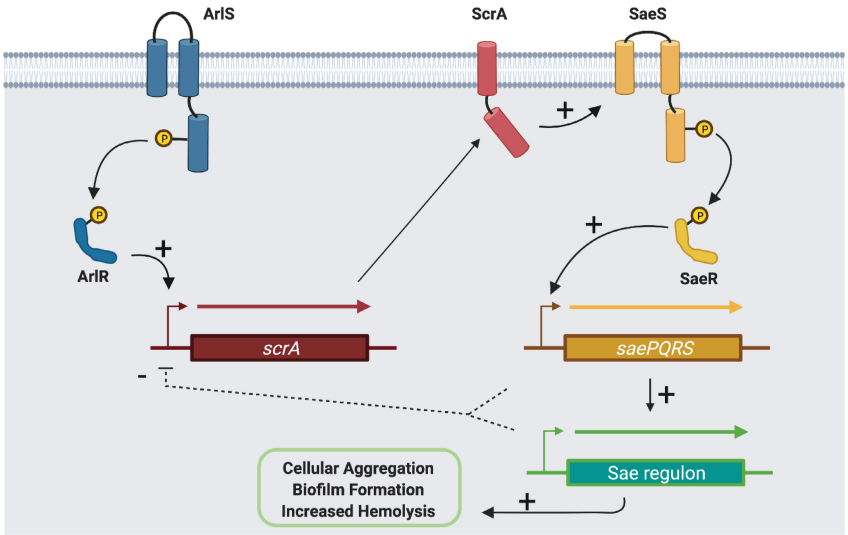

FIGURE 9 Hypothetical working model of ArlRS-ScrA-SaeRS action. ArlR positively regulates *scrA* expression, either directly or indirectly. The ScrA protein inserts into the cell membrane which in turn activates the SaeRS system, causing increased expression of Sae regulon genes. The increase in Sae system activity has a negative feedback on *scrA* expression either directly through SaeR or indirectly via a downstream Sae regulon gene

TABLE 1 Strains and plasmids used in this study

Strain or plasmid	Characteristics	Reference or source
S. aureus		
AH1263	USA 300 LAC isolate cured of plasmid LAC-p03	Boles et al. (2010)
RN4220	Restriction-deficient transformation recipient	Kreiswirth et al. (1983)
SH1000	*rbsU* repaired laboratory strain	Horsburgh et al. (2002)
UAMS-1	Osteomyelitis clinical isolate	Gillaspy et al. (1995)
Newman	Laboratory strain	Carroll et al. (2012)
RKC600	SH1000 pMK4	Zapf et al. (2019)
RKC602	UAMS-1 pMK4	Zapf et al. (2019)
RKC604	Newman pMK4	Zapf et al. (2019)
NE1622	JE2 *saeR*::Bursa, NARSA transposon mutant	Fey et al. (2013)
NE1296	JE2 *saeS*::Bursa, NARSA transposon mutant	Fey et al. (2013)
NE1684	JE2 *arlR*::Bursa, NARSA transposon mutant	Fey et al. (2013)
NE1532	JE2 *agrA*::Bursa, NARSA transposon mutant	Fey et al. (2013)
RKC681	AH1263 pRKC679	This study
RKC684	AH1263 *saeR*::Bursa	This study
RKC759	AH1263 pRKC751	This study
RKC760	AH1263 pRKC752	This study
RKC854	SH1000 pRKC752	This study
RKC856	Newman pRKC752	This study
RKC857	UAMS-1 pRKC752	This study
RKC878	AH1263 *saeR*::Bursa p*scrAB*	This study
RKC908	AH1263 *saeR*::Bursa pMK4_EV	This study
RKC1009	AH1263 pRKC1009	This Study
RKC1058	AH1263 pRKC1058	This Study
RKC1066	AH1263 *saeS*::Bursa p*scrAB*	This study
RKC1067	AH1263 *saeS*::Bursa pMK4_EV	This study
RKC1005	AH1263 pRKC993	This study
RKC1039	AH1263 pRKC1033	This study
RKC1040	AH1263 pRKC1034	This study
RKC809	AH1263 *arlR*::Bursa pMK4	This study
RKC0811	AH1263 *arlR*::Bursa pRKC752	This study
RKC0772	AH1263 *agrA*::Ery pRKC752	This study
RKC0694	AH1263 *agrA*::Ery	This study
RKC1229	AH1263 pRKC1226	This study
RKC1230	AH1263 pRKC1127	This study
E. coli		
DH5α	Cloning strain	Invitrogen
DH10β	Cloning strain	Invitrogen
Plasmids		
pMK4	Gram-positive shuttle vector (CM^R)	Sullivan et al. (1984)
pCN51	Cadmium inducible promoter (Ery^R)	Charpentier et al. (2004)
pRKC679	pMK4_p*scrA_6x-his* (vector overexpressing truncated his tagged *scrA* from its native promoter)	Sorensen et al. (2020)
pRKC751	pMK4_*scrA* (vector overexpressing full length *scrA* from its native promoter)	This Study
pRKC752	pMK4_*scrAB* (vector overexpressing *scrAB* from its native promoter)	This Study
pRKC993	pCN51_*scrAB* (vector overexpression *scrAB* from a cadmium inducible promoter)	This Study

TABLE 1 (Continued)

Strain or plasmid	Characteristics	Reference or source
pRKC1009	pMK4_*scrA*_TM (vector overexpressing the transmembrane domain of ScrA)	This Study
pRKC1033	pCN51_*scrA* (vector overexpressing *scrA* from a cadmium inducible promoter)	This Study
pRKC1034	pCN51_*scrB* (vector overexpressing *scrB* from a cadmium inducible promoter)	This Study
pRKC1058	pCN51_*scrA*_C-tail (vector overexpressing the c-terminal tail of ScrA from a cadmium inducible promoter)	This Study
pRKC1226	pCN51_*scrA*_NSAA3 (vector overexpressing *scrA* with a TAA nonsense mutation at amino acid 3 from a cadmium inducible promoter)	This Study
pRKC1227	pCN51_*scrA*_NSAA8 (vector overexpressing *scrA* with a TAA nonsense mutation at amino acid 8 from a cadmium inducible promoter)	This Study

fragment for pRKC993. Primers #1045/#1069 generated a fragment for pRKC1033. Primers #1070/#1071 generated a fragment for pRKC1034. The insert and backbone were restriction enzyme digested, the backbone was treated with alkaline phosphatase and the insert was ligated into the plasmid with T4 DNA ligase. Constructed plasmids were transformed into *Escherichia coli* strain DH5α. The creation of the *scrA* nonsense mutants was performed using an in vivo assembly (IVA) method as previously described (García-Nafría et al., 2016) using primer #1451/#1452 for pCN51_AA3 and #1453/#1454 for pCN51_AA8. Screening and sequencing to confirm insertion of the fragments into the vector utilized #0045/#0046 for pMK4 and #0230/#0231 for pCN51. Plasmids were introduced into *S. aureus* strain RN4220 by electroporation and phage transduced to strain AH1263.

4.2 | Bacterial growth conditions

S. aureus cultures were routinely grown at 37°C with shaking in tryptic soy broth (TSB). *E. coli* cultures were grown at 37°C with shaking in lysogeny broth (LB). Where indicated, antibiotics were used at the following concentrations: Chloramphenicol (10 μg/ml), erythromycin (5 μg/ml), lincomycin (25 μg/ml), ampicillin (100 μg/ml). Where indicated cultures were synchronized as follows. Five milliliters of overnight starter culture was diluted 1:100 into 10 ml of fresh, prewarmed TSB and grown for 3 h to mid-exponential phase. Cultures were then diluted into 25 ml of fresh TSB in a 250 ml flask to a starting OD_{600} of 0.05. Cultures were then grown for the indicated time.

4.3 | Bioinformatics analysis

CLC genomic workbench (Qiagen) was used for the analysis of RNA-seq data as described previously (Carroll et al., 2014). The previously published updated USA300 genome file was used as a reference for all RNA-seq analysis (Carroll et al., 2016). Volcano plots were generated as previously described (Briaud et al., 2021) using Rstudio V1.4.1106 (Team R Development Core, 2018) and the EnhancedVolcano package V1.8.0 with cutoffs set at log2 fold change >1 and $-\log_{10}$ *p*-value >1.3 (*p*-value <0.05).

4.4 | TCA precipitation

Nine milliliters of supernatant was combined with 1 ml of trichloroacetic acid and incubated at 4°C for 24 h. Precipitated proteins were pelleted at 4°C and washed three times with ice-cold acetone. The protein pellet was resuspended in 500 μl of 8 M urea unless otherwise noted.

4.5 | Cell clumping assay

Five milliliters of overnight cultures was grown at 37°C in a 15 ml conical tube. One milliliter of culture was transferred to a 1.7 ml microcentrifuge tube and pelleted. The cells were resuspended in phosphate-buffered saline (PBS) and thoroughly dispersed via vortex mixing and pipetting. One hundred microloters was removed from each tube and used to determine the initial OD_{600}. Suspensions were incubated statically at room temperature for 2 h. One hundred microliters of solution was removed from the top of the suspension and the OD_{600} was measured. The percent clumping was calculated as the percent reduction in OD_{600} after 2 h of incubation.

4.6 | Biofilm assay

Biofilm assays were modified from a previously described protocol by Cue et al. (2015). In short, each well in a 24-well cell culture-treated plate was coated with human serum as follows: 100 μl of 2% human serum was pipetted into each well and the plate was incubated overnight at 4°C. Human serum was aspirated from each well prior to inoculation with bacterial strains. Quadruplicate overnight bacterial cultures were diluted 1:100 into TSB supplemented with 0.5% dextrose and 3% NaCl. One milliliter of diluted culture was added to each well. Inoculated plates were incubated statically at 37°C for up to 6 h. At each timepoint, plates were removed and washed with 2x with PBS. Plates were baked at 60°C overnight to adhere biofilm to the wells. Biofilm was stained with 0.05% crystal violet and washed 2x with PBS. Biofilms were destained with acetic acid and the quantity of biofilm present in the wells was determined by measurement of OD_{595}.

TABLE 2 Oligonucleotides used in this study

Name	Sequence	Details
#0045	GTAAAACGACGGCCAGTG	M13 forward primer
#0046	GGAAACAGCTATGACCATG	M13 reverse primer
#0049	CCAACATTACAAGAGGTTGAACAAGC	*agr* R oligo
#0052	CGTATAATGACAGTGAGGAGAGTGG	*agrB* F
#0055	GGTAACAATAATCCAGTTATTGC	*arlR* F
#0056	CGTAATATGAGGTGTACAAATGACG	*arlR* R
#0057	CTAATTGATAACACCATTATCGG	*saeR* F
#0058	GAGGTCGTAAGAACAGAGG	*saeR* R
#0230	GGTGATGAACATATCAGGCAGA	pCN51 F
#0231	TGATATCAAAATTATACATGTCAACGA	pCN51 R
#0669	AAAACTGCAGAAAATTAATGCGATGATTTTTAGC	*scrA* His F
#0670	CGGATCCTTAATGATGATGATGATGATGATCTTTTGTCATGAAATAAATGGG	*scrA* His R
#0831	CGGATCCCCTGATAGAATATAATGTACTGTC	*scrA* rev
#0832	CGATCCCGCATAAATGATTCTATATTAATGC	*scrAB* rev
#0902	CAAGAGCTCcAAAATTAATGCGATGATTTTTAGC	*scrAB* F
#0972	AAAATCCGACAGTTCCAACG	*scrA* qPCR F
#0973	TGGGATGAATATCACGACTAGAAG	*scrA* qPCR R
#1045	ACGCgtcgacTTTTAGAAAGGATGTGAAA	*scrAB* into pCN51 F
#1046	GgaattcGCATAAATGATTCTATATTAATG	*scrAB* into pCN51 R
#1052	CGggatccTTAATGATGATGATGATGATGTTCATAATGTTTTGCATATTG	Truncated *scrA* into pMK4
#1069	GgaattcTTAATCTTTTGTCATGAAATAA	*scrA* into pCN51
#1070	ACGCgtcgacTATATTCTATCAGGAAGGTG	*scrB* into pCN51 F
#1071	GgaattcTTATGGGTATTTTGTAATTTTATAA	*scrB* into pCN51 R
#1129	ACGCgtcgacAGAAAGGATGTGAAATAATGCAATATGCAAAACATTATGA	*scrA* c-tail into pCN51 F
#1130	GgaattcTTAATCTTTTGTCATGAAATAAATG	*scrA* c-tail into pCN51 R
#1451	ATATTTTAGAAAGGATGTGAAATAATGAAATAATCTAAACAAATACTTTT GATTATGGGC	*scrA* TAA nonsense mutation at codon 3 in pCN51 F
#1452	TTTCATTATTTCACATCCTTTCTAAAATAT	*scrA* TAA nonsense mutation at codon 3 in pCN51 R
#1453	TGTGAAATAATGAAAGGCTCTAAACAAATATAATTGATTATGGGCATTATATC TCTTATTGT	*scrA* TAA nonsense mutation at codon 8 in pCN51 F
#1454	TATTTGTTTAGAGCCTTTCATTATTTCAC	*scrA* TAA nonsense mutation at codon 8 in pCN51 R
#1505	ATGAAAGGCTCTAAACAAATACTTTTGATTATGGGCATTA	*scrA* riboprobe F
#1506	TAATACGACTCACTATAGGGTTAATCTTTTGTCATGAAATAAATGGGATGAATATCAC GACTAGAAGTAATGTTA	*scrA* riboprobe R
#1507	TATATTCTATCAGGAAGGTGCAACAATGACC	*scrB* riboprobe F
#1508	TAATACGACTCACTATAGGGTTATGGGTATTTTGTAATTTTATAAAAG CAAACGTAGAATAATGCGATAAGTAATAATGC	*scrB* riboprobe R

4.7 | Sample preparation for proteomics

Synchronized 16 h cultures of *S. aureus* were centrifuged and the supernatant was filter sterilized. Secreted proteins were TCA precipitated as outlined above. Samples were prepared by filter-assisted sample preparation (FASP). Samples were resuspended in 4% (w/v) SDS, 100 mM Tris pH 7.4, 100 mM DTT, with protease inhibitor cocktail (ThermoFisher Scientific), clarified by centrifugation at 17,000×*g* for 10 min, and protein concentration was determined by Pierce 600 nm protein assay (ThermoFisher Scientific). Samples were then standardized to 100 μg and reduced at 37°C for 1 h. Urea was added to a final concentration of 6 M with 20 mM Tris pH 8.5, and samples were placed in a 30 kDa Mw protein concentrator column (Millipore Sigma). All centrifugation steps performed from this point were performed at 12,000×g for 3–5 min until column was almost empty. Three washes were performed with 8 M urea, 20 mM Tris pH 8.5 (urea buffer), prior

to alkylation with 10 mM iodoacetamide in urea buffer, and incubation in the dark at room temperature for 30 min. Washes were performed as above, followed by three more washes with 100 mM triethylammonium bicarbonate pH 8 (TEAB). Trypsin was added in TEAB at 1:100 trypsin: protein (1 μg), and incubated at 37°C for 18 h. Digested samples were eluted by centrifugation, desalted using C18 columns (Waters), and resuspended in 2% ACN 0.1% formic acid.

4.8 | Mass spectrometry and data analysis

Digested peptides (5 μl) were separated on a 50 cm Acclaim™ PepMap™ 100 C18 reversed-phase high-pressure liquid chromatography (HPLC) column (Thermo Fisher Scientific) using an Ultimate3000 UHPLC (Thermo Fisher Scientific) with a 60 (in-gel digest) or 180 (whole proteome) min gradient (2% to 32% acetonitrile with 0.1% formic acid). Peptides were analyzed on a hybrid Quadrupole-Orbitrap instrument (Q Exactive Plus; Thermo Fisher Scientific) using data-dependent acquisition in which the top 10 most abundant ions were selected for MS/MS analysis. Raw files were searched against the *S. aureus* USA300 proteome (UniProt ID: UP000001939) using MaxQuant (Cox & Mann, 2008) (www.maxquant.org) and the integrated Andromeda search engine. Digestion was set as trypsin/P, variable modifications included oxidation (M) and acetylation (protein N-term), and carbamidomethylation (C) was fixed. Label-free quantification was used, with peptides matched between runs. Other settings were left as defaults. The resulting protein groups files were further processed using Perseus (Tyanova et al., 2016), and for whole proteome experiments, this included an imputation step with default settings. Unpaired *t*-test with Welch's correction was used to establish significant changes in protein abundance (LFQ intensity) between strains. Proteins with a *p*-value less than 0.05 and a fold change greater than 2 up or down were considered significant. The mass spectrometry proteomics data have been deposited to the ProteomeXchange Consortium via the PRIDE (REF - PubMed ID: 30395289) partner repository with the dataset identifier PXD028409.

4.9 | Human erythrocyte lysis assay

Measurement of human erythrocyte lysis was performed as previously described (Keogh et al., 2019). In short, 16 h cell-free supernatants were diluted 1:2 in a reaction buffer consisting of 40 mM $CaCl_2$ and 1.7% NaCl. Twenty-five microliters of whole human blood was added to the solution. Samples were incubated at 37°C while rotating. Intact erythrocytes were pelleted at 5500 × *g* and the OD_{543} of the supernatant was recorded. Samples were averaged to either the WT strain or empty vector as indicated.

4.10 | RNA isolation

Samples for RNA-sequencing were prepared as follows. Triplicate cultures were synchronized and grown for 3 h. Five milliliters of bacterial culture was pelleted and washed with ice-cold PBS. Pellets were stored at −80°C until use. Isolation of RNA was performed as previously described (Hussein et al., 2019) using a slightly modified protocol for the RNeasy mini prep kit (Qiagen). RNA samples were treated with a Turbo DNA Free Kit (Ambion). RNA integrity was confirmed via Bioanalyzer (Agilent 2100 Bioanalyzer) and all samples had RIN values >9. RNA was stored at −80°C until use.

4.11 | RNA sequencing

Ribosomal RNA depletion was performed on each sample using a *Staphylococcus aureus*-specific riboPOOL rRNA removal kit (siTOOLs Biotech). RNAseq libraries were generated from the rRNA-depleted samples by the Ohio University Genomics Facility. Libraries were created using the Illumina TruSeq Stranded mRNA kit (Illumina Cat. # 20020594) per the manufacturer's instruction starting with the Fragment, Prime, and Finish step to accommodate non-polyadenylated, rRNA-depleted bacterial RNA. Resultant libraries were sequenced on the Illumina MiSeq using Illumina MiSeq Reagent Kit v3 (150 cycle) (Illumina Cat# MS-102-3001) to generate 75 bp paired-end reads. RNA-seq data are deposited in the Gene Expression Omnibus (GEO) database under the accession number GSE184753.

4.12 | Propidium iodide assay

Bacterial cultures were pelleted and resuspended to an OD_{600} of 1.5. One milliliter of culture was washed with PBS and 100 μl was transferred to a 96 well plate. One microliter of propidium iodide was added to the remaining 900 μl of culture and allowed to incubate statically at room temperature for 5 min. One hundred microliters of culture was then moved to a 96 well plate. Fluorescence was measured with an excitation wavelength of 535 nm and an emission wavelength of 617 nm.

4.13 | Reverse transcriptase-quantitative PCR (RT-qPCR)

Biological quadruplicates were grown and 1 μg total RNA was reverse transcribed using the iScript cDNA synthesis kit (BioRad) per manufacturer instruction. cDNA was diluted 10 times and qPCR was performed using iTaq Universal SYBR Green Supermix (BioRad) in technical duplicates. The housekeeping gene *gyrB* was used as an endogenous control in all reactions. Amplification and analysis were performed as previously described (Fris et al., 2017).

4.14 | Northern blot

RNA was isolated from cultures grown for 3 h as described above. The quantity and purity of the RNA were determined by a bioanalyzer

nanochip. Either 10 or 20 μg of RNA were loaded onto a formaldehyde agarose gel and electrophoresed for 1 h 15 m at 120 V. The gel was transferred to a nylon membrane by capillary transfer and RNA was UV cross-linked to the membrane. The ladder and rRNA bands were visualized by staining with a 0.04% methylene blue and 0.5 M sodium acetate solution. To detect the *scrAB* transcript(s) a riboprobe was synthesized as follows: a PCR fragment encompassing either the *scrA* or *scrB* open reading frame was synthesized containing a T7 promoter driving antisense expression of *scrA* or *scrB*. This fragment was used as template in an in vitro transcription reaction to generate an antisense riboprobe. The probe was synthesized using α-P^{32}-labeled cytosine triphosphate. The membrane was prehybridized for 2 h at 68°C prior to the addition of the probe. The probe was allowed to hybridize overnight at 68°C. The membrane was washed with 2X SSC, 1X SSC, and 0.5X SSC, for 15 min each at 68°C. The membrane was exposed to a phosphor imaging screen overnight and visualized using a phosphor imager.

ACKNOWLEDGMENTS

We acknowledge the support and expertise provided by the Ohio University Genomics Facility in the completion of the RNA library preparation and MiSeq sequencing, and support from Dale Chaput and the USF proteomics core for assistance with mass spectrometry. This work was supported by grant AI156391 from the National Institute of Allergy and Infectious Diseases (NIAID) to RKC and in part by grants AI124458 and AI157506 from NIAID to LNS. The authors declare no conflict of interests.

ETHICS APPROVAL

Human blood was obtained in accordance with procedures approved by the Ohio University Institutional Review Board. Blood was obtained from anonymous donors at Ohio University.

DATA AVAILABILITY STATEMENT

The data that support the findings of this study are openly available in GEO at https://www.ncbi.nlm.nih.gov/geo/, reference number GSE184753, and the PRIDE database at https://www.ebi.ac.uk/pride/archive/, reference number PXD028409.

ORCID

Ronan K. Carroll https://orcid.org/0000-0001-7090-3414

REFERENCES

Adhikari, R.P. & Novick, R.P. (2008) Regulatory organization of the staphylococcal sae locus. *Microbiology*, *154*, 949–959. https://doi.org/10.1099/mic.0.2007/012245-0

Boles, B.R., Thoendel, M., Roth, A.J. & Horswill, A.R. (2010) Identification of genes involved in polysaccharide-independent *Staphylococcus aureus* biofilm formation. *PLoS One*, *5*, e10146. https://doi.org/10.1371/JOURNAL.PONE.0010146

Briaud, P., Frey, A., Marino, E.C., Bastock, R.A., Zielinski, R.E., Wiemels, R.E. et al. (2021) Temperature influences the composition and cytotoxicity of extracellular vesicles in *Staphylococcus aureus*. *mSphere*, *6*, e00676-21. https://doi.org/10.1128/mSphere.00676-21

Bronesky, D., Wu, Z., Marzi, S., Walter, P., Geissmann, T., Moreau, K. et al. (2016) *Staphylococcus aureus* RNAIII and its regulon link quorum sensing, stress responses, metabolic adaptation, and regulation of virulence gene expression. *Annual Review of Microbiology*, *70*, 299–316. https://doi.org/10.1146/annurev-micro-102215-095708

Carroll, R.K., Robison, T.M., Rivera, F.E., Davenport, J.E., Jonsson, I.M., Florczyk, D. et al. (2012) Identification of an intracellular M17 family leucine aminopeptidase that is required for virulence in *Staphylococcus aureus*. *Microbes and Infection*, *14*, 989–999. https://doi.org/10.1016/j.micinf.2012.04.013

Carroll, R.K., Weiss, A., Broach, W.H., Wiemels, R.E., Mogen, A.B., Rice, K.C. et al. (2016) Genome-wide annotation, identification, and global transcriptomic analysis of regulatory or small RNA gene expression in *Staphylococcus aureus*. *MBio*, *7*, e01990-15. https://doi.org/10.1128/mBio.01990-15.Invited

Carroll, R.K., Weiss, A. & Shaw, L.N. (2014) RNA-sequencing of *Staphylococcus aureus* messenger RNA. *Methods in Molecular Biology*, *1373*, 131–141. https://doi.org/10.1007/7651_2014_192

Charpentier, E., Anton, A.I., Barry, P., Alfonso, B., Fang, Y. & Novick, R.P. (2004) Novel cassette-based shuttle vector system for gram-positive bacteria. *Applied and Environmental Microbiology*, *70*, 6076–6085. https://doi.org/10.1128/AEM.70.10.6076-6085.2004

Cho, H., Jeong, D.-W., Liu, Q., Yeo, W.-S., Vogl, T., Skaar, E.P. et al. (2015) Calprotectin increases the activity of the SaeRS two component system and murine mortality during *Staphylococcus aureus* infections. *PLoS Pathogens*, *11*, e1005026. https://doi.org/10.1371/journal.ppat.1005026

Claes, J., Liesenborghs, L., Peetermans, M., Veloso, T.R., Missiakas, D., Schneewind, O. et al. (2017) Clumping factor a, von Willebrand factor-binding protein and von Willebrand factor anchor *Staphylococcus aureus* to the vessel wall. *Journal of Thrombosis and Haemostasis*, *15*, 1009–1019. https://doi.org/10.1111/jth.13653

Cox, J. & Mann, M. (2008) MaxQuant enables high peptide identification rates, individualized p.p.b.-range mass accuracies and proteome-wide protein quantification. *Nature Biotechnology*, *26*, 1367–1372. https://doi.org/10.1038/nbt.1511

Crosby, H.A., Tiwari, N., Kwiecinski, J.M., Xu, Z., Dykstra, A., Jenul, C. et al. (2020) The *Staphylococcus aureus* ArlRS two-component system regulates virulence factor expression through MgrA. *Molecular Microbiology*, *113*, 103–122. https://doi.org/10.1111/mmi.14404

Cue, D., Junecko, J.M., Lei, M.G., Blevins, J.S., Smeltzer, M.S. & Lee, C.Y. (2015) SaeRS-dependent inhibition of biofilm formation in *Staphylococcus aureus* Newman. *PLoS One*, *10*, e0123027. https://doi.org/10.1371/journal.pone.0123027

Fey, P.D., Endres, J.L., Yajjala, V.K., Widhelm, T.J., Boissy, R.J., Bose, J.L. et al. (2013) A genetic resource for rapid and comprehensive phenotype screening of nonessential *Staphylococcus aureus* genes. *MBio*, *4*, e00537–e00512. https://doi.org/10.1128/MBIO.00537-12

Fris, M., Broach, W., Klim, S., Coschigano, P., Carroll, R.K., Caswell, C. et al. (2017) Sibling sRNA RyfA1 influences shigella dysenteriae pathogenesis. *Genes*, *8*, 50. https://doi.org/10.3390/genes8020050

Garai, P. & Blanc-Potard, A. (2020) Uncovering small membrane proteins in pathogenic bacteria: regulatory functions and therapeutic potential. *Molecular Microbiology*, *114*, 710–720. https://doi.org/10.1111/mmi.14564

García-Nafría, J., Watson, J.F. & Greger, I.H. (2016) IVA cloning: a single-tube universal cloning system exploiting bacterial in vivo assembly. *Scientific Reports*, *6*, 1–12. https://doi.org/10.1038/srep27459

Geiger, T., Goerke, C., Mainiero, M., Kraus, D. & Wolz, C. (2008) The virulence regulator Sae of *Staphylococcus aureus*: promoter activities and response to phagocytosis-related signals. *Journal of Bacteriology*, *190*, 3419–3428. https://doi.org/10.1128/JB.01927-07

Gillaspy, A.F., Hickmon, S.G., Skinner, R.A., Thomas, J.R., Nelson, C.L. & Smeltzer, M.S. (1995) Role of the accessory gene regulator (agr) in pathogenesis of staphylococcal osteomyelitis.

Infection and Immunity, *63*, 3373–3380. https://doi.org/10.1128/iai.63.9.3373-3380.1995

Giraudo, A.T., Cheung, A.L. & Nagel, R. (1997) The sae locus of *Staphylococcus aureus* controls exoprotein synthesis at the transcriptional level. *Archives of Microbiology*, *168*, 53–58. https://doi.org/10.1007/s002030050469

Haag, A.F. & Bagnoli, F. (2015) The role of two-component signal transduction systems in *Staphylococcus aureus* virulence regulation. *Current Topics in Microbiology and Immunology*, *409*, 145–198. https://doi.org/10.1007/82_2015_5019

Horsburgh, M.J., Aish, J.L., White, I.J., Shaw, L., Lithgow, J.K. & Foster, S.J. (2002) SigmaB modulates virulence determinant expression and stress resistance: characterization of a functional rsbU strain derived from staphylococcus. *Journal of Bacteriology*, *184*, 5457–5467. https://doi.org/10.1128/JB.184.19.5457-5467.2002

Hussein, H., Fris, M.E., Salem, A.H., Wiemels, R.E., Bastock, R.A., Righetti, F. et al. (2019) An unconventional RNA-based thermosensor within the 5′ UTR of *Staphylococcus aureus* cidA. *PLoS One*, *14*, e0214521. https://doi.org/10.1371/journal.pone.0214521

Janzon, L., Löfdahl, S. & Arvidson, S. (1989) Identification and nucleotide sequence of the delta-lysin gene, hld, adjacent to the accessory gene regulator (agr) of *Staphylococcus aureus*. *MGG Molecular & General Genetics*, *219*, 480–485. doi:10.1007/BF00259623

Jenul, C. & Horswill, A.R. (2019) Regulation of *Staphylococcus aureus* virulence. *Microbiology Spectrum*, *7*, e7.2.29. https://doi.org/10.1128/microbiolspec.gpp3-0031-2018

Jeong, D.-W., Cho, H., Jones, M.B., Shatzkes, K., Sun, F., Ji, Q. et al. (2012) The auxiliary protein complex SaePQ activates the phosphatase activity of sensor kinase SaeS in the SaeRS two-component system of *Staphylococcus aureus*. *Molecular Microbiology*, *86*, 331–348. https://doi.org/10.1111/j.1365-2958.2012.08198.x

Jin, Z., Jiang, Q., Fang, B. & Sun, B. (2019) The ArlR-MgrA regulatory cascade regulates PIA-dependent and protein-mediated biofilm formation in Rbf-dependent and Rbf-independent pathways. *International Journal of Medical Microbiology*, *309*, 85–96. https://doi.org/10.1016/j.ijmm.2018.12.006

Keogh, R.A., Zapf, R.L., Trzeciak, E., Null, G.G., Wiemels, R.E. & Carroll, R.K. (2019) Novel regulation of alpha-toxin and the phenol-soluble Modulins by peptidyl-prolyl cis/trans isomerase enzymes in *Staphylococcus aureus*. *Toxins*, *11*, 343. https://doi.org/10.3390/toxins11060343

Kluytmans, J., van Belkum, A. & Verbrugh, H. (1997) Nasal carriage of *Staphylococcus aureus*: epidemiology, underlying mechanisms, and associated risks. *Clinical Microbiology Reviews*. *American Society for Microbiology*, *10*, 505–520. https://doi.org/10.1128/cmr.10.3.505-520.1997

Kreiswirth, B.N., Löfdahl, S., Betley, M.J., O'Reilly, M., Schlievert, P.M., Bergdoll, M.S. et al. (1983) The toxic shock syndrome exotoxin structural gene is not detectably transmitted by a prophage. *Nature*, *305*, 709–712. https://doi.org/10.1038/305709a0

Kwiecinski, J.M., Crosby, H.A., Valotteau, C., Hippensteel, J.A., Nayak, M.K., Chauhan, A.K. et al. (2019) *Staphylococcus aureus* adhesion in endovascular infections is controlled by the ArlRS–MgrA signaling cascade. *PLoS Pathogens*, *15*, e1007800. https://doi.org/10.1371/journal.ppat.1007800

Lalaouna, D., Baude, J., Wu, Z., Tomasini, A., Chicher, J., Marzi, S. et al. (2019) RsaC sRNA modulates the oxidative stress response of *Staphylococcus aureus* during manganese starvation. *Nucleic Acids Research*, *47*, 9871–9887. https://doi.org/10.1093/nar/gkz728

Liesenborghs, L., Meyers, S., Lox, M., Criel, M., Claes, J., Peetermans, M. et al. (2019) *Staphylococcus aureus* endocarditis: distinct mechanisms of bacterial adhesion to damaged and inflamed heart valves. *European Heart Journal*, *40*, 3248–3259. https://doi.org/10.1093/eurheartj/ehz175

Liu, Q., Yeo, W. & Bae, T. (2016) The SaeRS two-component system of *Staphylococcus aureus*. *Genes*, *7*, 81. https://doi.org/10.3390/genes7100081

Mäder, U., Nicolas, P., Depke, M., Pané-Farré, J., Debarbouille, M., van der Kooi-Pol, M.M. et al. (2016) *Staphylococcus aureus* transcriptome architecture: from laboratory to infection-mimicking conditions. *PLoS Genetics*, *12*, 1005962. https://doi.org/10.1371/journal.pgen.1005962

Mainiero, M., Goerke, C., Geiger, T., Gonser, C., Herbert, S. & Wolz, C. (2010) Differential target gene activation by the *Staphylococcus aureus* two-component system saeRS. *Journal of Bacteriology*, *192*, 613–623. https://doi.org/10.1128/JB.01242-09

Miravet-Verde, S., Ferrar, T., Espadas-García, G., Mazzolini, R., Gharrab, A., Sabido, E. et al. (2019) Unraveling the hidden universe of small proteins in bacterial genomes. *Molecular Systems Biology*, *15*, e8290. https://doi.org/10.15252/msb.20188290

Nielsen, J.S., Christiansen, M.H.G., Bonde, M., Gottschalk, S., Frees, D., Thomsen, L.E. et al. (2011) Searching for small σb-regulated genes in *Staphylococcus aureus*. *Archives of Microbiology*, *193*, 23–34. https://doi.org/10.1007/s00203-010-0641-1

Párraga Solórzano, P.K., Yao, J., Rock, C.O. & Kehl-Fie, T.E. (2019) Disruption of glycolysis by nutritional immunity activates a two-component system that coordinates a metabolic and antihost response by *Staphylococcus aureus*. *MBio*, *10*, e01321-19. https://doi.org/10.1128/mBio.01321-19

Rapun-Araiz, B., Haag, A.F., de Cesare, V., Gil, C., Dorado-Morales, P., Penades, J.R. et al. (2020) Systematic reconstruction of the complete two-component sensorial network in *Staphylococcus aureus*. *mSystems*, *5*, e00511-20. https://doi.org/10.1128/msystems.00511-20

Rogasch, K., Rühmling, V., Pané-Farré, J., Höper, D., Weinberg, C., Fuchs, S. et al. (2006) Influence of the two-component system SaeRS on global gene expression in two different *Staphylococcus aureus* strains. *Journal of Bacteriology*, *188*, 7742–7758. https://doi.org/10.1128/JB.00555-06

Romilly, C., Caldelari, I., Parmentier, D., Lioliou, E., Romby, P. & Fechter, P. (2012) Current knowledge on regulatory RNAs and their machineries in *Staphylococcus aureus*. *RNA Biology*, *9*, 402–413. https://doi.org/10.4161/rna.20103

Schilcher, K., Caesar, L.K., Cech, N.B. & Horswill, A.R. (2020) Processing, export, and identification of novel linear peptides from *Staphylococcus aureus*. *MBio*, *11*, e00112-20. https://doi.org/10.1128/mBio.00112-20

Sorensen, H.M., Keogh, R.A., Wittekind, M.A., Caillet, A.R., Wiemels, R.E., Laner, E.A. et al. (2020) Reading between the lines: Utilizing RNA-Seq data for global analysis of sRNAs in *Staphylococcus aureus*. *mSphere*, *5*, e00439-20. https://doi.org/10.1128/mSphere.00439-20

Sullivan, M.A., Yasbin, R.E. & Young, F.E. (1984) New shuttle vectors for *Bacillus subtilis* and *Escherichia coli* which allow rapid detection of inserted fragments. *Gene*, *29*, 21–26. https://doi.org/10.1016/0378-1119(84)90161-6

Team R Development Core. A language and environment for statistical computing . Vienna, Austria: R Foundation for Statistical Computing; 2018. https://www.R-project.org

Tong, S.Y.C., Davis, J.S., Eichenberger, E., Holland, T.L. & Fowler, V.G. (2015) *Staphylococcus aureus* infections: epidemiology, pathophysiology, clinical manifestations, and management. *Clinical Microbiology Reviews*, *28*, 603–661. https://doi.org/10.1128/CMR.00134-14

Tyanova, S., Temu, T., Sinitcyn, P., Carlson, A., Hein, M.Y., Geiger, T. et al. (2016) The Perseus computational platform for comprehensive analysis of (prote)omics data. *Nature Methods*, *13*, 731–740. https://doi.org/10.1038/nmeth.3901

Wang, R., Braughton, K.R., Kretschmer, D., Bach, T.-H.L., Queck, S.Y., Li, M. et al. (2007) Identification of novel cytolytic peptides as key virulence determinants for community-associated MRSA. *Nature Medicine*, *13*, 1510–1514. https://doi.org/10.1038/nm1656

Wertheim, H.F.L., Melles, D.C., Vos, M.C., van Leeuwen, W., van Belkum, A., Verbrugh, H.A. et al. (2005) The role of nasal carriage in *Staphylococcus aureus* infections. *Lancet Infectious Diseases*, *5*, 751–762. https://doi.org/10.1016/S1473-3099(05)70295-4

Zapf, R.L., Wiemels, R.E., Keogh, R.A., Holzschu, D.L., Howell, K.M., Trzeciak, E. et al. (2019) The small RNA Teg41 regulates expression of the alpha phenol-soluble Modulins and is required for virulence in *Staphylococcus aureus*. *MBio*, *10*, e02484-18. https://doi.org/10.1128/mBio.02484-18

SUPPORTING INFORMATION

Additional supporting information may be found in the online version of the article at the publisher's website.

How to cite this article: Wittekind, M. A., Frey, A., Bonsall, A. E., Briaud, P., Keogh, R. A., Wiemels, R. E., Shaw, L. N. & Carroll, R. K. (2022). The novel protein ScrA acts through the SaeRS two-component system to regulate virulence gene expression in *Staphylococcus aureus*. *Molecular Microbiology*, *117*, 1196–1212. https://doi.org/10.1111/mmi.14901